Supplementary Information

Reaction kinetics of meteoric sodium reservoirs in the upper atmosphere

J. C. Gómez Martín, S. A. Garraway and J. M. C Plane*

School of Chemistry, University of Leeds, Woodhouse Lane, LS2 9JT, Leeds, UK

* J.M.C.Plane@leeds.ac.uk

Contents:

A. FIGURES

Figure S1

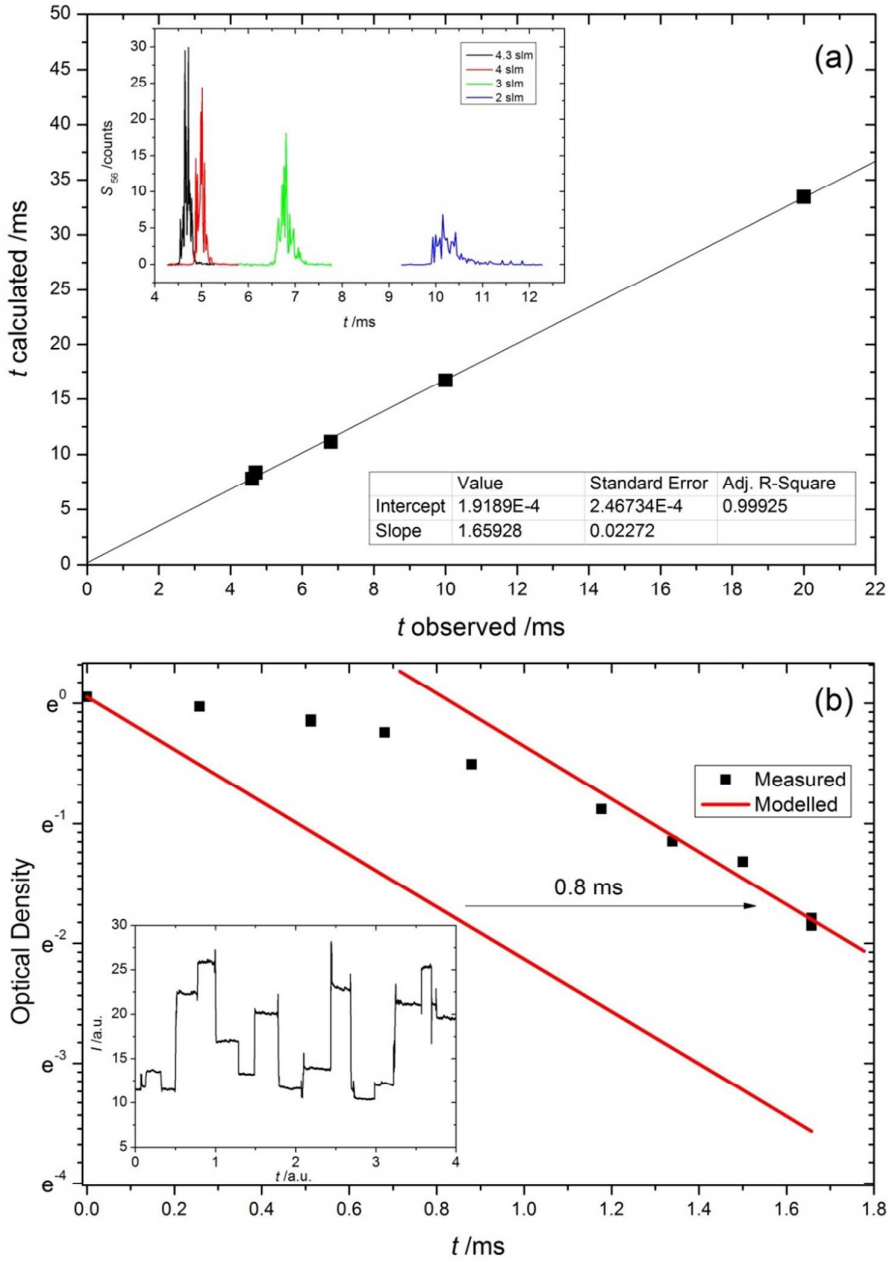

Figure S1 Characterization of contact time between reactants: (a) The insert panel shows ablated Fe pulses travelling down the flow tube at different linear speeds (pulses become lower and wider due to radial and axial diffusion, respectively). The observed peak arrival time is plotted vs. the calculated flow time, where the slope of the linear regression yields the parabolic velocity profile correction factor; (c) Na continuously released from the furnace reacts with constant $[N_2O]= 8 \times 10^{14}$ molecule cm^{-3}, injected at different distances to the Na resonance absorption detection point (P = 1 Torr). The insert panel shows the change in 589 nm transmitted intensity with varying N_2O injection point (the contact time between reagents is changed between 0 and 1.7 ms). Mixing time caused by off-axis N_2O injection results in Na reaching the expected decay rate after 0.8 ms.

Figure S2

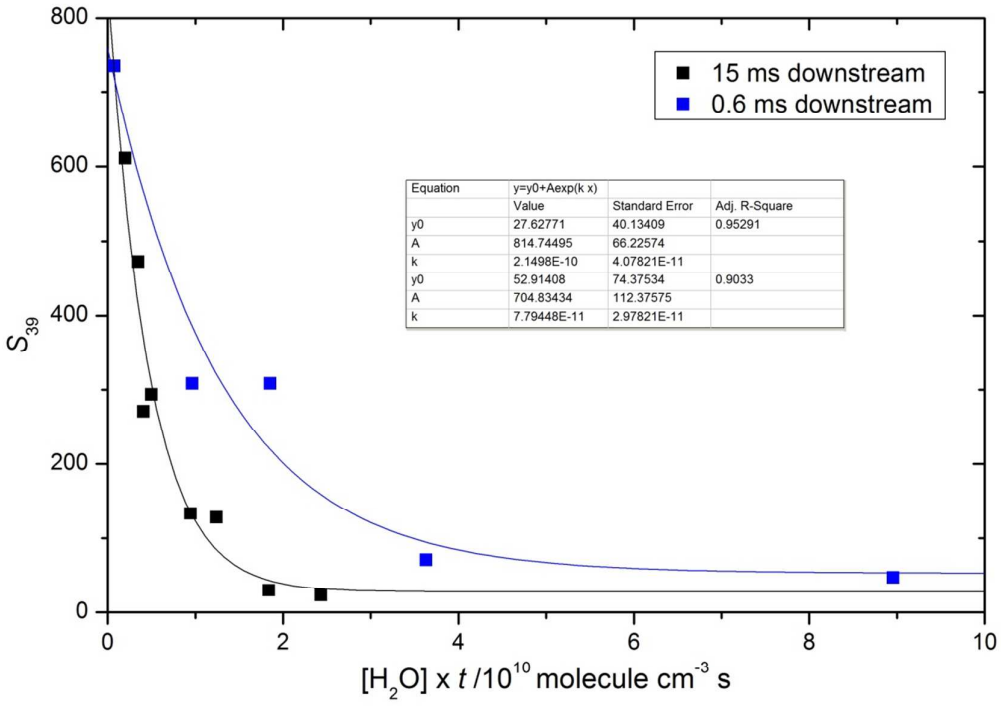

Figure S2. Decay of S_{39} with increasing $[H_2O]$ for injection close (0.6 ms downstream) and far (15 ms downstream) from the source chemistry (blue and black squares respectively).

Figure S3

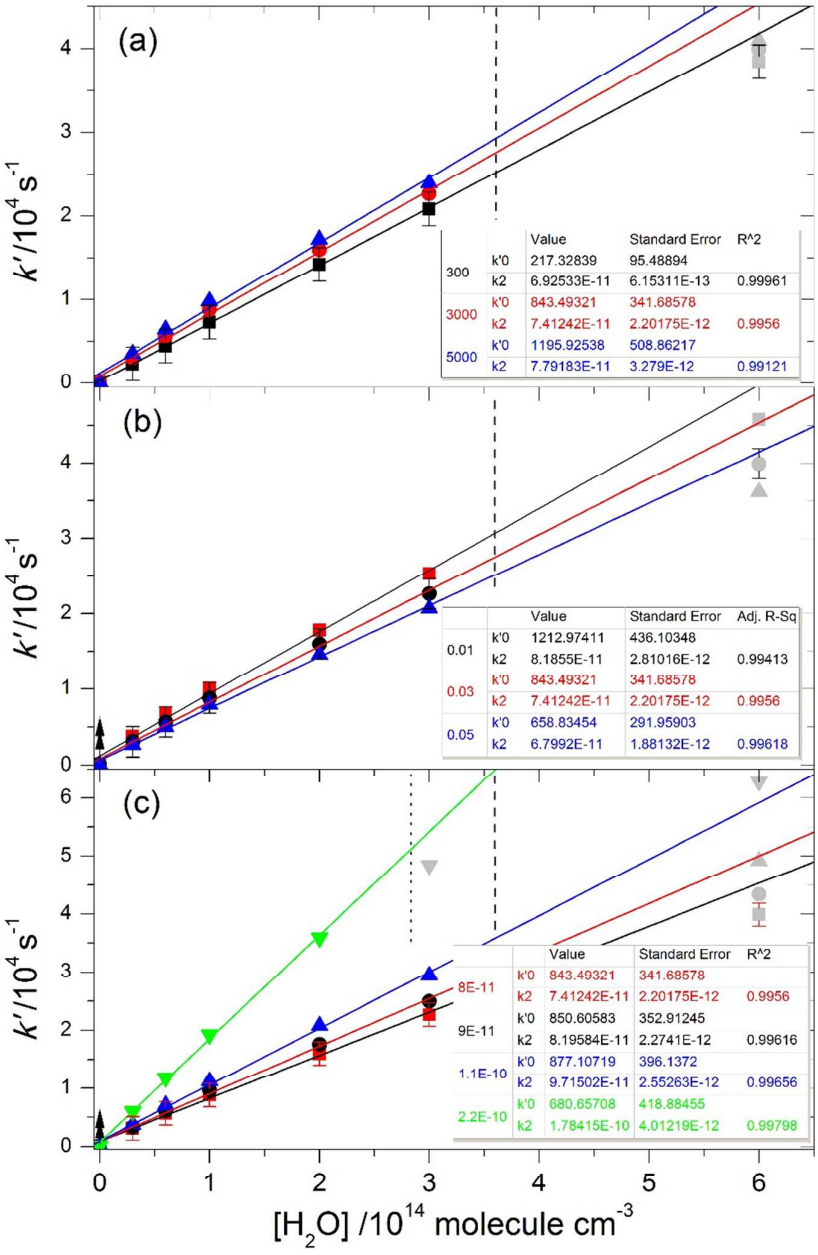

Figure S3. Bimolecular plots for simulations of the NaO removal by reaction with H_2O in the PLP-chemiluminescence system employed by Cox and Plane.[1] The retrieved values of k_2(A) are shown in the tables. Panel (a): simulations at constant NaO(A) quenching rate (3000 s^{-1}) and N_2O photolysed fraction (0.03%), for different values of k_2(A) assumed in the numerical model. Panel (b): simulations at constant k_2(A) (8×10^{-11} cm^3 $molecule^{-1}$ s^{-1}) and N_2O photolysed fraction (0.03%), for different values of the NaO(A) quenching rate. Panel (c): simulations at constant NaO(A) quenching rate (3000 s^{-1}) and k_2(A) (8×10^{-11} cm^3 $molecule^{-1}$ s^{-1}), for different values of the N_2O photolysed fraction. The grey squares are data outside the linear section of the bimolecular plots, as defined by the uncertainty in Cox and Plane's experimental data. Vertical dashed and dotted lines: highest $[H_2O]$ in Cox and Plane's bimolecular plots for high temperature and room temperature, respectively.

Figure S4

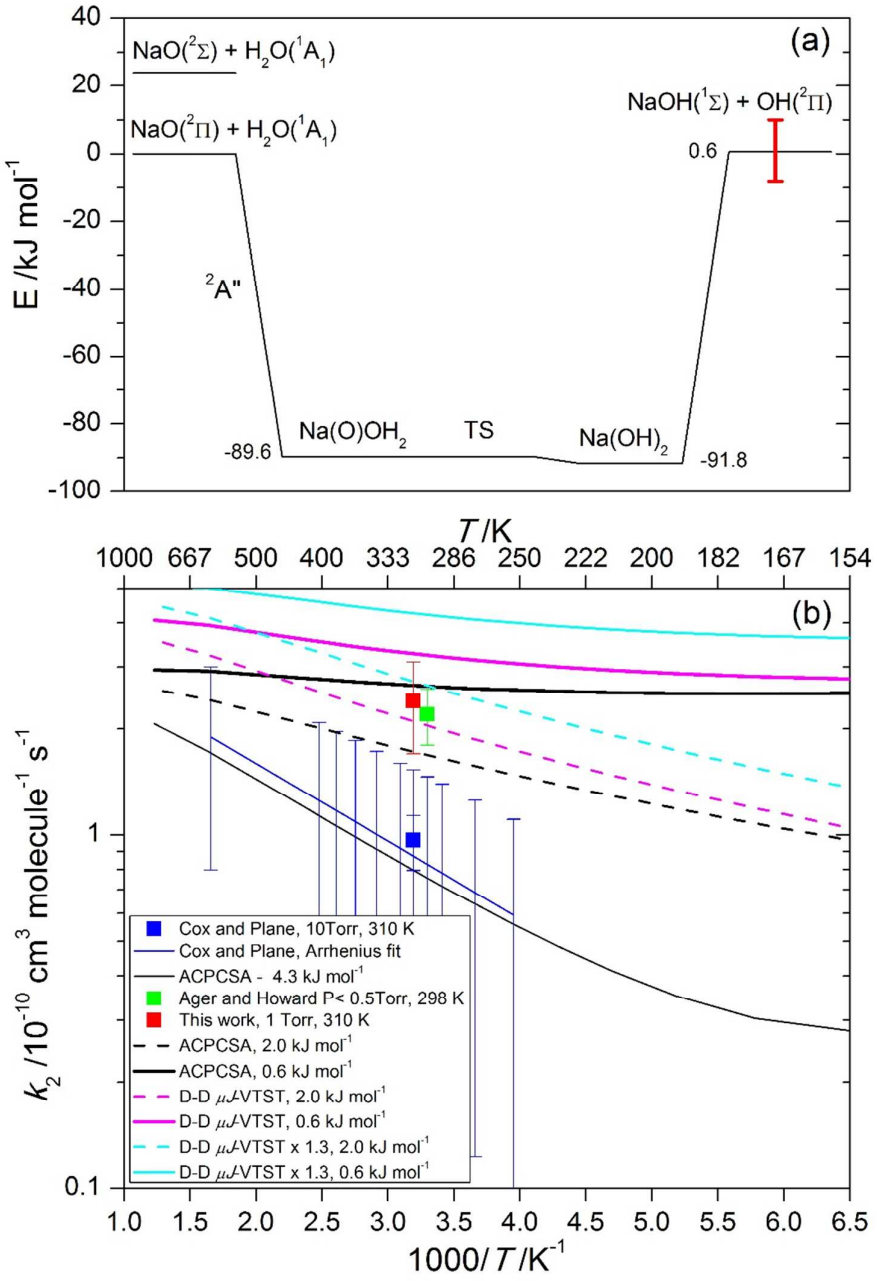

Figure S4. Panel (a): Potential energy surface for the NaO + H_2O reaction at CBS-QB3 level (0 K).[2] The red error bar indicates the experimental uncertainty of the enthalpy of reaction. [3-5] Panel (b): comparison of experimental determinations of $k(NaO+H_2O)$ [1, 6] (square symbols, and blue line) with statistical rate theory calculations using MESMER [7] with ΔH_r^0 from the CBS-QB3 calculations (0.6 kJ mol^{-1}, thick lines) or adjusted to 2 kJ mol^{-1} [8, 9] (dashed lines) and 4.3 kJ mol^{-1} [1] (thin black line). Following Cox and Plane,[1] some of the master equation calculations consider the NaO + H_2O ACPCSA rate constant from Stoecklin and Clary[10] as an estimate of the high pressure limit rate constant (black lines). The magenta and cyan lines correspond calculations where the high pressure limit is estimated from the μJ-VTST dipole-dipole expression by Georgievskii and Klippenstein [11] (in the case of the cyan lines multiplied by a factor of 1.3 to account for other long range effects, Table S5).

Figure S5

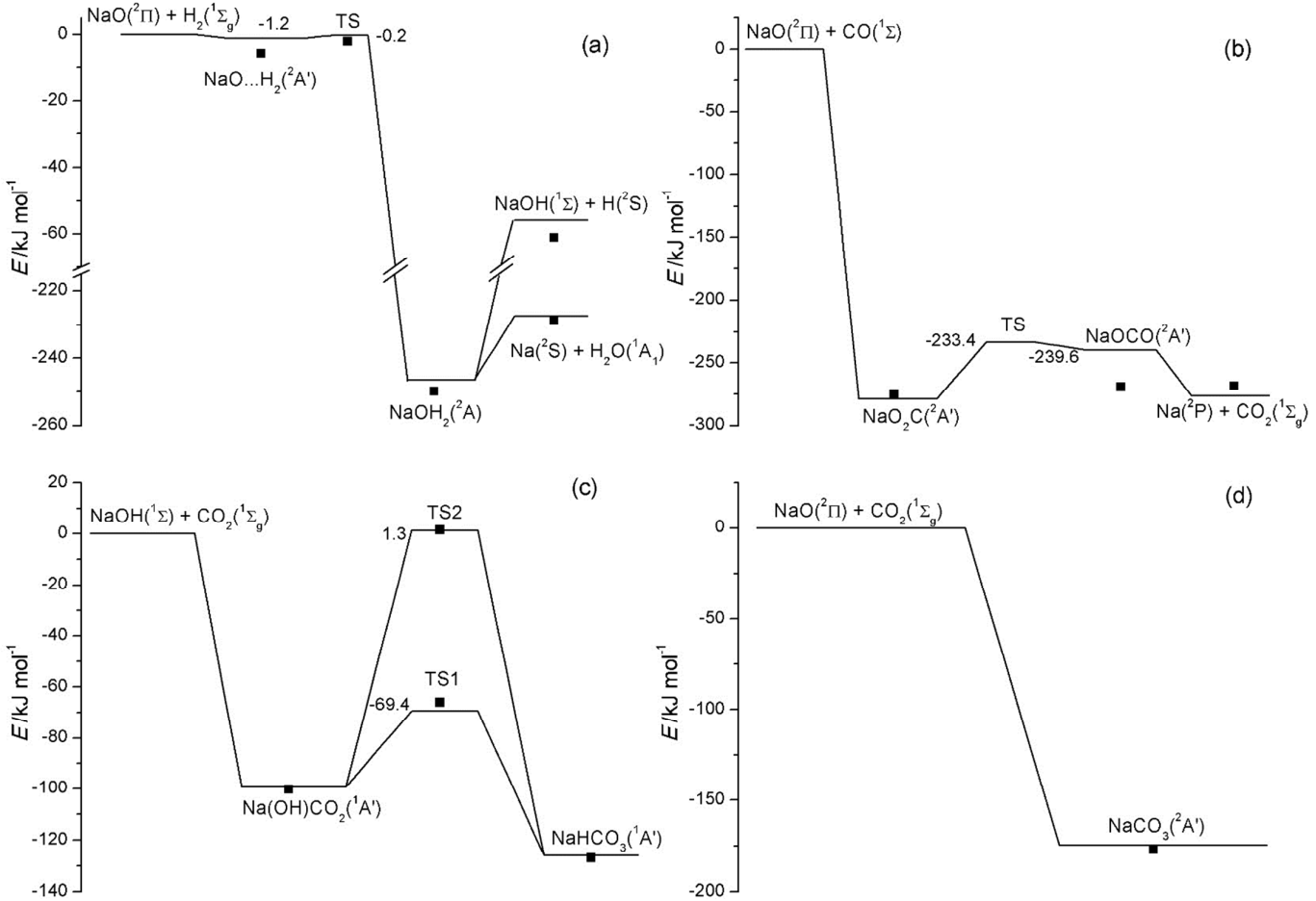

Figure S5. Stationary points of the ground state potential energy surfaces from CBS-QB3 calculations for (a) NaO + H_2 (a) , NaO + CO (b), NaOH + CO_2 (c), and NaO+CO_2 (d). Symbols refer to W1U calculations.

Figure S6

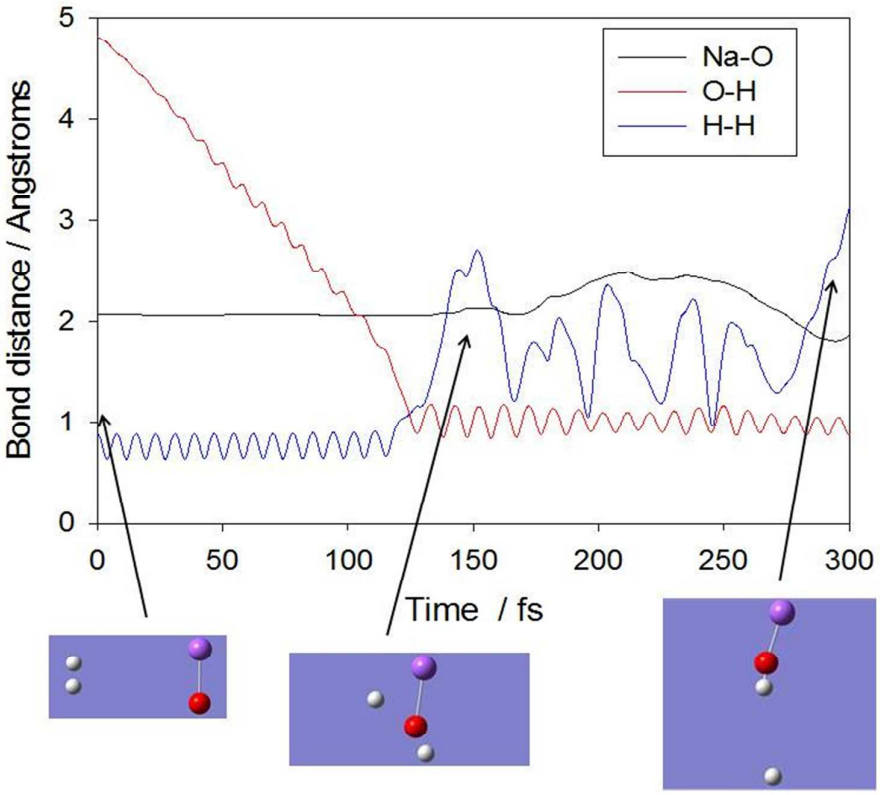

Figure S6. Example of classical trajectory calculation for the NaO + H_2 reaction at 300 K using B3LYP /6-311G+(2d,p) level of theory and the Atom Centred Density Matrix Propagation molecular dynamics model. Collisions are not always reactive. Reactive collisions require a small impact parameter and they always result in NaOH + H products.

Figure S7

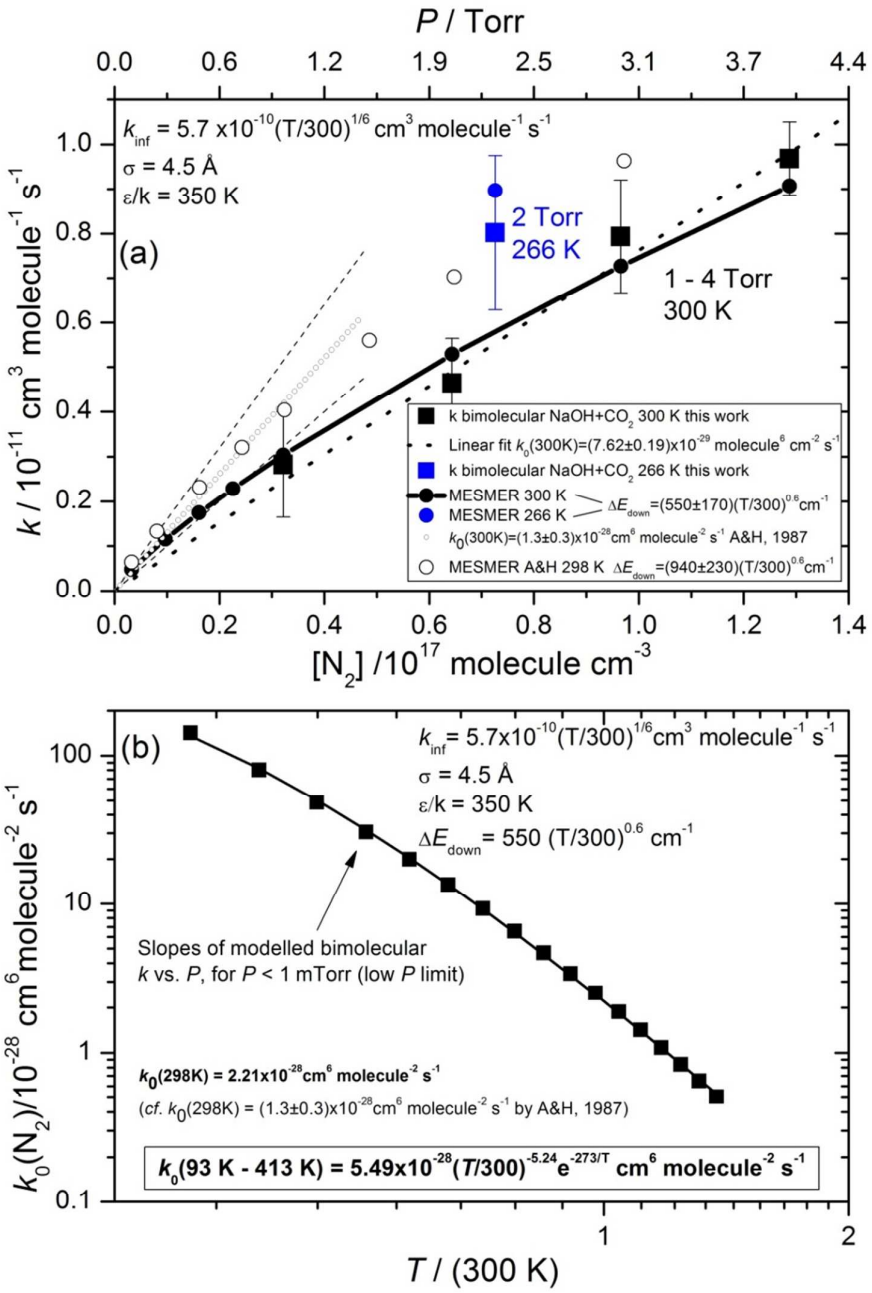

Figure S7. Master equation modelling/fitting and extrapolation of rate constants for R4. Panel (a): MESMER modelling of observed bimolecular rate constants for the NaOH + CO_2 reaction. The squares correspond to the data obtained in the present study (black: 300 K, blue: 266 K). A linear fit of this dataset (thick dotted line) is shown for comparison with Ager and Howard's[12] third order rate constant (small circles, uncertainty range indicated by thin dashed lines). MESMER modelled and fitted bimolecular rate constants are shown by circles: Full circles (black: 298 K, blue: 266 K) for the fit to the present study's data, empty circles for the fit to Ager and Howard's values. Panel (b): temperature dependence of the low pressure limit rate constants obtained from MESMER using the parameters required to model the observations of the present study (squares in the top panel). The solid line corresponds represents an empirical fit of the modelled k_0 vs. T curve to a modified Arrhenius expression (optimal parameters indicated inside the box).

Figure S8

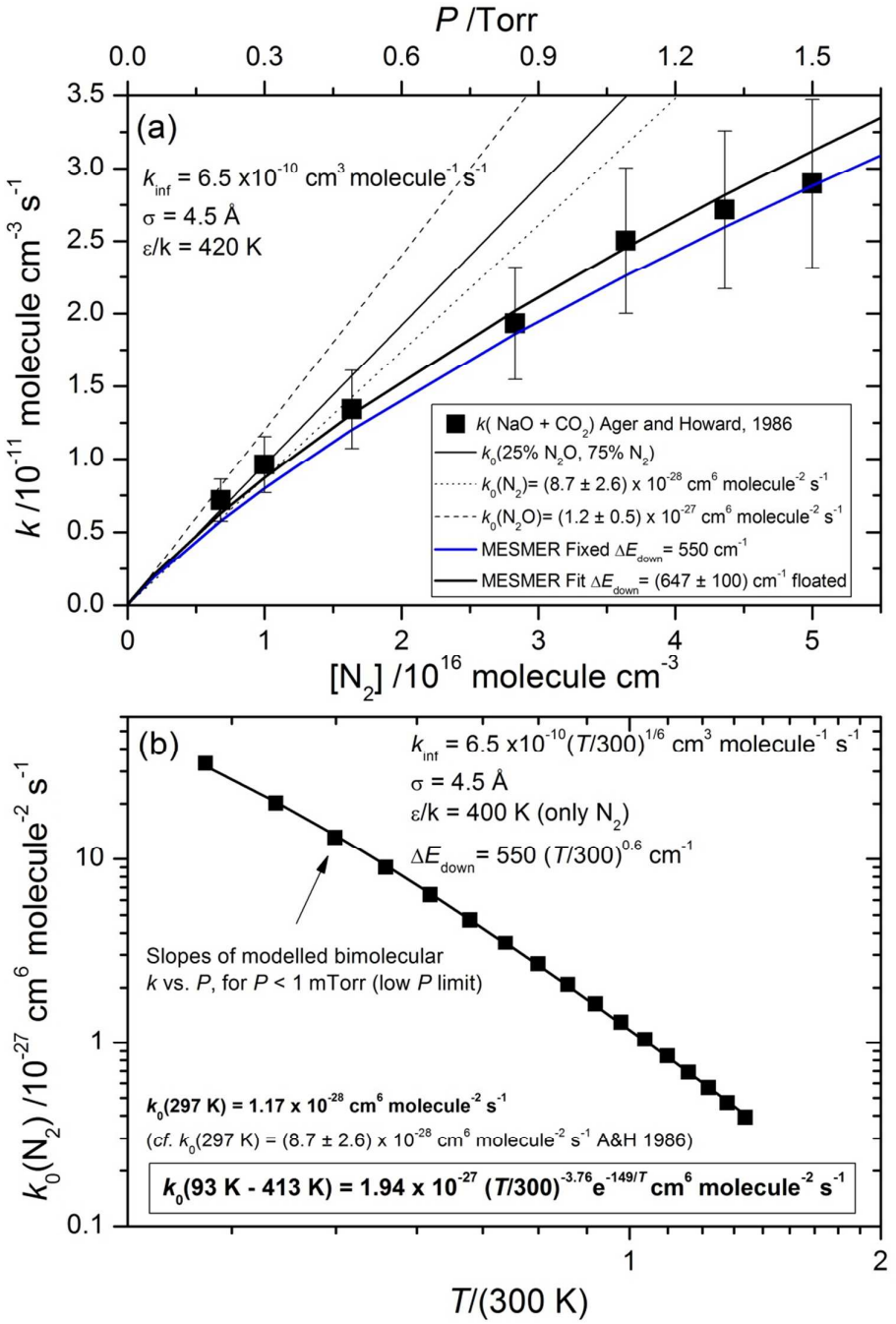

Figure S8. Master equation modelling/fitting and extrapolation of rate constants for R5. Panel (a): MESMER modelling of observed bimolecular rate constants for the NaO + CO_2 reaction. The squares correspond to the experimental data in Fig. 2 of the paper by Ager and Howard.[13] Third order rate constants are indicated by the dashed, solid and dotted black lines (N_2O, N_2O/N_2 mixture and N_2 respectively). MESMER modelled and fitted bimolecular rate constants are shown by a solid black curve. The blue curve shows modelled rate constants for the optimal value of ΔE_{down} for R4. Panel (b): temperature dependence of the low pressure limit rate constants obtained from MESMER using the parameters required to model the observations of Ager and Howard (squares in the top panel). The solid line corresponds represents an empirical fit of the modelled k_0 vs. T curve to a modified Arrhenius expression (optimal parameters indicated inside the box).

B. Discussion of the results for the NaO+H_2O reaction by Cox and Plane[1] (Figure S3)

In the flow tube experiments reported in this paper, the quenching rate needs to be at least 300 s^{-1} to relax all the $A^2\Sigma$ state in the flow tube experiment prior to detection, which results in a lower limit for the N_2 quenching rate constant of ~1×10^{-14} cm^3 $molecule^{-1}$ s^{-1}. In Cox and Plane's experiments at 10 Torr, this would correspond to a quenching rate of 3000 s^{-1}. Numerical modelling of Cox and Plane's PLP experiments has been carried out in order to assess the impact of NaO($A^2\Sigma$) quenching on their results. The chemical model described in Table S1 is used to generate an ordinary differential equations system (ODES) which is numerically integrated using one of Matlab's built-in ODES solvers (ode15s). The resulting modelled chemiluminescence decays as a function of time are then analysed in a pseudo-first order fashion, extracting the decay rates and finally generating bi-molecular plots of these as a function of [H_2O].

The bimolecular plots in Fig S3a show that a quenching rate of the NaO($A^2\Sigma$) state of a 3000 s^{-1} causes an increase of the NaO loss rate with respect to a slow quenching scenario (300 s^{-1}), but this is within the experimental uncertainty (~25% at 300 K). In addition, the bimolecular plot remains linear within the water concentration range considered by Cox and Plane. Therefore, k(NaO($A^2\Sigma$)+N_2) ~ 1×10^{-14} cm^3 $molecule^{-1}$ s^{-1} is compatible with both Cox and Plane's and our observations.

This modelling exercise also reveals that the chemiluminescent reactions R9-R10 could have interfered slightly with the chemistry under study if the N_2O photolysed fraction was as large as quoted (0.03 - 0.05%). This would have generated a pool of Na atoms which would be have been converted to NaO in the same time scale of the NaO + H_2O reaction, thus slowing down the loss of NaO, e.g. by about 16% for 0.05% N_2O photolysis (Fig. S3b). Since the N_2O photolysis was variable throughout the PLP experiments, this is a potential cause of the

relatively large scatter observed in the Arrhenius plot. Fig. S3c also shows that for an average N_2O photolysis fraction of 0.03%, a rate constant for NaO + H_2O as fast as 2×10^{-10} cm^3 molecule^{-1} s^{-1} would cause significant curvature in the bimolecular plot for [H_2O] $\geq 3 \times 10^{14}$ molecule cm^3, which is higher than the upper limit of Cox and Plane's water concentration range at high temperature (700 K).

In summary, modelling supports the idea that –with a few caveats- Cox and Plane's approach was appropriate, but also that it is perfectly possible that the rate constant of the NaO + H_2O reaction they measured refers to the NaO($A^2\Sigma$) state.

C. TABLES

Table S1. Numerical model of Cox and Plane's PLP-LIF experiments on the NaO + H_2O reaction at 298 K

Reaction [a]	***k'* /s^{-1} or *k*/ cm^3 molecule^{-1} s^{-1}**	**Ref.**
NaOH + hν → Na + OH	Instantaneous	
N_2O + hν → N_2 + O(^{1}D)	Instantaneous, 0.03-0.05% photolysis	
O(^{1}D) + N_2 → O(^{3}P)+N_2	3.110×10^{-10}	14
O(^{1}D) + H_2O → OH + OH	1.994×10^{-10}	14
Na(^{2}S) + N_2O → NaO(A) + N_2	1.3×10^{-12}	14
NaO(A) + N_2 → NaO(X) + N_2	300 – 5000	Varied
NaO(X) + O(^{3}P) → Na(^{2}S) + O_2	3.145×10^{-10}	15, 16
NaO(X) + O(^{3}P) → Na(^{2}P$_J$) + O_2	0.555×10^{-10}	15, 16
NaO(A) + O(^{3}P)→ Na(^{2}S) + O_2	4.386×10^{-10}	17
NaO(A) + O(^{3}P)→Na(^{2}P$_J$) + O_2	0.714×10^{-10}	17
Na(^{2}P$_J$)→Na(^{2}S) + hν_{589nm}	Instantaneous	
NaO(X) + H_2O → NaOH + OH	2.2×10^{-10}	6
NaO(A) + H_2O → NaOH + OH	$0.8 \times 10^{-10} – 2.2 \times 10^{-10}$	Varied

[a] Diffusional losses[18] also included, but irrelevant for pseudo-first order kinetic analysis in PLP experiments.

Table S2. Optimized geometries of the ground states of relevant sodium-containing species at B3LYP/6-311+G(2d,p) level of theory.

Species	**State**	**Cartesian coordinates /Å**			
NaO	$^2\Pi$	Na	0.000000	0.000000	0.000000
		O	0.000000	0.000000	2.067900
NaOH	$^1\Sigma$	O	0.000000	0.000000	-1.021042
		Na	0.000000	0.000000	0.926010
		H	0.000000	0.000000	-1.975968
$NaO\ldots H_2$	$^2A'$	Na	0.008553	0.000000	0.004005
		O	-0.001963	0.000000	2.070636
		H	2.639545	0.000000	1.941855
		H	1.930061	0.000000	2.207671
$NaOH_2$ TS [a]	$^2A'$	Na	-0.015800	0.000000	-0.012820
		O	0.021454	0.000000	2.053866
		H	2.147190	0.000000	1.523684
		H	1.456665	0.000000	1.960312
$Na\ldots OH_2$	^2A	O	-1.165053	0.000001	-0.033600
		H	-1.729083	-0.775068	0.108177
		H	-1.729099	0.775057	0.108178
		Na	1.161691	0.000000	0.004768
$Na\ldots O_2C$	$^2A'$	Na	-0.000006	-1.391713	0.000000
		O	1.131821	0.560534	0.000000
		O	-1.131814	0.560515	0.000000
		C	0.000000	1.056743	0.000000
$NaCO_2$ TS [a]	$^2A'$	Na	1.727171	-0.504218	0.000000
		O	0.000000	1.028779	0.000000
		O	-1.607702	-0.631849	0.000000
		C	-1.022878	0.395159	0.000000
$Na\ldots CO_2$	$^2A'$	Na	2.322112	-1.228785	0.000000
		O	0.000000	0.658108	0.000000
		O	-2.320419	0.567430	0.000000
		C	-1.163314	0.618722	0.000000
$Na(O)OH_2$	$^2A''$	Na	-0.067625	0.000000	-0.102042
		O	0.068111	0.000000	2.081133
		H	1.397548	0.000000	1.407442
		O	2.022043	0.000000	0.549499
		H	2.947509	0.000000	0.801046
$Na(OH)_2$ TS [b]	$^2A''$	Na	0.074294	0.000000	-0.048386
		O	0.105955	0.000000	2.207271
		H	1.225378	0.000000	1.677971
		O	2.021271	0.000000	0.773276
		H	2.940274	0.000000	1.043159
$Na(OH)_2$	$^2A''$	Na	-0.097083	0.000000	-0.247158
		O	0.222026	0.000000	2.050218
		H	1.134545	0.000000	1.512506
		O	1.902323	0.000000	0.265673
		H	2.859678	0.000000	0.239638

$NaCO_3$	$^2A'$	C	0.000000	0.007211	-0.513104
		O	0.000000	-0.027286	0.753708
		O	0.000000	1.080005	-1.187535
		O	0.000000	-1.109152	-1.149804
		Na	0.000000	2.202023	0.737334
$Na(OH)CO_2$	$^1A'$	C	-0.119330	0.000000	0.029535
		O	-0.117161	0.000000	1.527580
		O	1.059825	0.000000	-0.390452
		O	-1.216078	0.000000	-0.482156
		Na	2.071187	0.000000	1.509282
		H	-1.045221	0.000000	1.788507
$NaHCO_3$ TS1 [a,c]	$^1A'$	C	-0.456242	0.267308	0.048064
		O	0.071040	-0.578230	1.027822
		O	0.079041	0.077299	-1.089322
		O	-1.330300	1.059265	0.369181
		Na	1.151773	-0.521578	-2.660222
		H	-0.405963	-0.343773	1.834511
$NaHCO_3$ TS2 [a,c]	$^1A'$	C	0.087169	0.000000	0.208408
		O	0.098312	0.000000	1.576660
		O	1.120848	0.000000	-0.473836
		O	-1.163487	0.000000	-0.101885
		Na	2.290745	0.000000	1.398733
		H	-1.089895	0.000000	1.198953
$NaHCO_3$	$^1A'$	C	0.105035	0.323949	-0.371566
		O	-0.009128	1.171385	0.858514
		O	-0.165621	1.013439	-1.380562
		O	0.425356	-0.826315	-0.174581
		Na	-0.566835	2.880658	-0.386502
		H	0.211193	0.589683	1.595296
Na_2	$^1\Sigma_g$	Na	0.000000	0.000000	0.000000
		Na	0.000000	0.000000	3.051500
Na_2O	$^1\Sigma_g$	O	0.000000	0.000000	0.000000
		Na	0.000000	0.000000	1.987406
		Na	0.000000	0.000000	-1.987406

[a] See Fig. S5. [b] Fig. S4.[c] TS1: Na atom migration, TS2: H atom migration.

Table S3. Molecular parameters of relevant species at B3LYP/6-311+G(2d,p) level of theory.

Species	**M**	**State**	**E 0K/H** [a]	**μ_D /Debye**	**α/ Å^3**	**Rot. Constants /cm^{-1}**	**Vibr. Frequencies /cm^{-1}**
H_2	2	$^1\Sigma_g$	-1.1695030	0	0.4490 [*0.8059*]	60.408	4419.3
H_2O	18	$^1A'$|	-76.4382358	2.082 [*1.854* [b]]	1.12 [*1.45*]	27.5374, 14.284, 9.405	1618.6, 3811.1, 3915.5
CO	28	$^1\Sigma$	-113.3469765	0.10 [*0.11*]	1.83 [*1.95*]	1.9404	2210.5
CO_2	44	$^1\Sigma_g$	-188.6389849	0	2.315 [*2.911*]	0.3914	675.8, 675.8, 1364.2, 2400.0
N_2	28	$^1\Sigma_g$	-109.5579322	0	1.6140 [*1.7403*]	2.0210	2435.6
N_2O	44	$^1\Sigma$	-184.7132485	0.100 [*0.161*]	2.64 [*3.03*]	0.4221	611.0, 611.0, 2317.0
Na	23	^2S	-162.2867797	0	[*2.36*]		
NaO	39	$^2\Pi$	-237.4770718	7.935	3.727	0.4180	478.8
NaOH	40	$^1\Sigma$	-238.1579210	6.585	2.950	0.4204	218.3, 218.3, 560.9, 3963.5
NaO…H_2	41	$^2A'$	-238.6480704	7.8734	4.288	1.7805, 0.3836, 0.3156	49.2, 90.2, 222.6, 476.8, 554.2, 4144.7
$NaOH_2$ TS [c]	41	$^2A'$	-238.6482048	7.5778	4.570	2.7650, 0.3981, 0.3480	-524.5, 154.8, 474.2,474.2, 910.1, 3012.9
Na…OH_2	41	$^2A'$	-238.7351135	2.7169	34.293	13.4948, 0.2892 ,0.2835	81.2, 225.2, 242.3, 1606.4, 3683.2, 3791.6
Na…O_2C	67	$^2A'$	-350.9288379	6.9422	7.327	0.4114, 0.2481, 0.1548	231.9, 290.4, 306.8, 738.5, 1252.0, 1690.9
$NaCO_2$ TS [c]	67	$^2A'$	-350.9154951	3.6842	22.923	0.5577, 0.1368, 0.1098	-253.3, 98.5, 302.8, 327.0, 1175.5, 2082. 8
Na…OCO	67	$^2A'$	-350.9261573	0.9281	26.568	1.7744, 0.0629, 0.0607	26.4, 28.3, 645.1, 652.5, 1354.6, 2388.7
Na(O)OH_2	57	$^2A''$	-313.9506248	5.9668	3.774	0.3704, 0.3132, 0.1697	175.7, 230.2, 302.9, 432.5,

							676.7, 830.0, 1530.5, 2238.6, 3910.7
$Na(OH)_2$ TS [d]	57	$^2A''$	-313.9534581	5.7889	3.735	0.3548, 0.3425, 0.1743	-591.7, 239.0, 338.2, 383.2, 630.0, 687.4, 873.7, 1697.9, 3924.5
$Na(OH)_2$	57	$^2A''$	-313.9525956	5.6227	4.544	0.3730, 0.3141, 0.1705	194.9, 245.0, 294.4, 450.4, 502.0, 630.1, 1200.6, 2118.1, 3926.9
$NaCO_3$	83	$^2A'$	-426.1845576	8.709	5.278	0.4220, 0.1156, 0.0907	80.9, 220.3, 307.8, 364.3, 623.1, 823.6, 1053.7, 1273.6, 1445.6
$Na(OH)CO_2$	84	$^1A'$	-426.8314826	9.4615	4.808	0.3816, 0.1122, 0.0867	90.2, 249.6, 333.7, 493.4, 529.6, 615.9, 784.5, 798.1, 1148.6, 1275.2, 1843.4, 3833.9
$NaHCO_3$ TS1 [c,e]	84	$^1A'$	-426.8174664	10.546	4.940	0.4026, 0.0766, 0.0644	-42.9, 44.9, 361.6, 569.5, 583.8, 653.7, 822.7, 968.4, 1232.6, 1361.1, 1756.9, 3804.8
$NaHCO_3$ TS2 [c,e]	84	$^1A'$	-426.7915454	8.6047	4.741	0.3846, 0.1168, 0.0896	-1858.3, 101.6, 246.7, 322.3, 641.8, 749.0, 811.3, 1040.4, 1102.0, 1357.8, 1672.7, 2239.6
$NaHCO_3$	84	$^1A'$	-426.8404242	6.766	4.737	0.4101, 0.1115, 0.0877	109.2, 248.9, 335.0, 570.7, 581.1, 700.2, 832.7, 1008.0, 1237.5, 1388.8, 1658.7, 3802.8
Na_2	46	$^1\Sigma_g$	-324.6004889	0	34.0 [*38.5*]	0.1575	159.8
Na_2O	62	$^1\Sigma_g$	-399.8370590	0	14.632	0.0930	33.9, 33.9, 353.9, 676.9

[a] 0 K, ZPE corrected. [b] Experimental values in brackets, from the Handbook of Chemistry and Physics.[19] Only experimental values for magnitudes required in calculations of long range capture rate constant are included in the table. [c] See Fig. S5. [d] Fig. S4.[e] TS1: Na atom migration, TS2: H atom migration.

Table S4. ZPE-corrected total energies at 0K and enthalpies at 298 K at the CBS-QB3 and W1U levels of theory (in Hartrees).

Species	**CBS-QB3**		**W1U**	
	E (0 K) /H	**H (298 K) /H**	**E (0 K) /H**	**H (298 K) /H**
H	-0.49981800	-0.49745700	-0.49999400	-0.49763400
H_2	-1.16608300	-1.16277800	-1.16467500	-1.16137100
O	-74.9876290	-74.9852690	-75.1113200	-75.1089600
O_2	-150.164605	-150.161297	-150.410767	-150.407459
OH	-75.6497220	-75.6464170	-75.7739590	-75.7706540
H_2O	-76.3374880	-76.3337080	-76.4620690	-76.4582900
CO	-113.182008	-113.178703	-113.372998	-113.369693
CO_2	-188.372093	-188.368520	-188.685512	-188.681941
N_2	-109.398465	-109.395161	-109.580173	-109.576869
N_2O	-184.450805	-184.447173	-184.752951	-184.749328
Na	-161.845983	-161.843623	-162.325686	-162.323326
NaO	-236.930750	-236.927221	-237.535920	-237.532380
NaOH	-237.618290	-237.613604	-238.223889	-238.219146
NaO…H_2	-238.097270	-238.091526	-238.702753	-238.696686
$NaOH_2$ (TS)	-238.096951	-238.092020	-238.701363	-238.696434
Na…OH_2	-238.190665	-238.18531	-238.795773	-238.790152
Na…O_2C	-350.219003	-350.213746	-351.01364	-351.008387
NaOCO TS	-350.201652	-350.196391		
Na…OCO	-350.204031	-350.198301	-351.0	-351.005751
$Na(O)OH_2$	-313.302354	-313.296569	-314.033320	-314.027480
$Na(OH)_2$ TS	-313.304371	-313.299112	-314.035512	-314.030185
$Na(OH)_2$	-313.303150	-313.297304	-314.034590	-314.028666
$NaCO_3$	-425.369350	-425.363262	-426.288897	-426.282773
$Na(OH)CO_2$	-426.028256	-426.022077	-426.947616	-426.941406
$NaHCO_3$ TS1	-426.016381	-426.010811	-426.934555	-426.928932
$NaHCO_3$ TS2	-425.989226	-425.983474	-426.908849	-426.903064
$NaHCO_3$	-426.038348	-426.032397	-426.957749	-426.951773
Na_2	-323.719118	-323.715184	-324.678165	-324.674226
Na_2O	-398.856481	-398.851063	-399.942318	-399.936873

Table S5. Enthalpies of reaction and Bond dissociation energies (in kJ mol^{-1}) obtained using the CBS-QB3 and W1U methods.

	CBS-QB3		**W1U**		**ΔH_r(298 K) Other theory** [a]		**Exp. ΔH_r(298)** [d]
Reaction	**ΔH_r(0 K)**	**ΔH_r(298 K)**	**ΔH_r(0 K)**	**ΔH_r(298 K)**	**W*n*C** [b]	**CCSD(T)/CBS** [c]	
$Na + N_2O \rightarrow NaO + N_2$	-85.1	-82.9	-98.3	-96.1	-103.0	-99.0	-102 ± 4
$Na_2 + N_2O \rightarrow Na_2O + N_2$	-223.2	-220.2	-239.9	-236.8	-249.1	-245.9	-260 ± 8
$NaO + H_2 \rightarrow NaOH + H$	-55.9	-55.3	-61.1	-60.5	-59.2	-55.4	-60 ± 9
$NaO + H_2 \rightarrow Na + H_2O$	-227.5	-229.3	-228.8	-230.7	-220.9	-224.9	-222 ± 4
$NaO + H_2O \rightarrow NaOH + OH$	0.6	2.4	0.4	2.3	2.0	1.8	1 ± 9
$NaO + CO \rightarrow Na + CO_2$	-276.5	-278.9	-268.5	-270.9	-262.1	-266.0	-263 ± 4
$NaO + CO_2 \rightarrow NaCO_3$	-174.6	-177.3	-177.1	-179.7			
$NaOH + CO_2 \rightarrow NaHCO_3$	-125.9	-132.0	-126.9	-133.1			
Dissociation							
$NaO \rightarrow Na + O$		258.2		262.8	270.1	266.1	270 ± 4
$NaOH \rightarrow Na + OH$		324.4		328.6	335.5	331.8	342 ± 8
$NaOH \rightarrow NaO + H$		496.0		496.5	492.1	495.4	496 ± 9

[a] From published ab initio enthalpies of formation and bond dissociation energies of NaO, NaOH, and Na_2O, and the well know experimental enthalpies of formation of H, OH, H_2O, CO, CO_2, N_2O, Na and Na_2. [b] From Mintz et al.[9] [c] From Vasiliu et al.[8] [d] Enthalpies of formation at 298 K: ΔH_f(Na) = (107.3 ± 0.7) kJ mol^{-1}, $\Delta H_f(Na_2)$ = (142.1 ± 1.0) kJ mol^{-1}, ΔH_f(H) = (217.998 ± 0.010) kJ mol^{-1} and $\Delta H_f(N_2O)$ = (82.05 ± 0.4) kJ mol^{-1} (JANAF tables [20]); ΔH_f(CO) = (-110.54 ± 0.17) kJ mol^{-1} and $\Delta H_f(CO_2)$ = (-393.51 ± 0.13) kJ mol^{-1} (CODATA[21]); ΔH_f(OH) = (37.36 ± 0.13) kJ mol^{-1} and $\Delta H_f(H_2O)$ = (-241.81 ± 0.03) kJ mol^{-1} (Ruscic et al.[4]); ΔH_f(NaOH) = (-191 ± 8) kJ mol^{-1} (Gurvich [5]); ΔH_f(NaO) = (87 ± 4) kJ mol^{-1} and $\Delta H_f(Na_2O)$ = (-36 ± 8) kJ mol^{-1} (Steinberg and Schofield [3]).

Table S6. Long range attraction rate coefficients (300 K)

Interaction	***k* (Dipole-Dipole) /10^{-10} cm^3 molecule^{-1} s^{-1}**			***k* (Dipole-Ind. Dipole) /10^{-10} cm^3 molecule^{-1} s^{-1}**		***k* (Dispersion) /10^{-10} cm^3 molecule^{-1} s^{-1}**	
System	*London* [a]	ACIOSA [b]	μ*J*-VTST [d]	*London* [a]	μ*J*-VTST [d]	*London* [a]	μ*J*-VTST [d]
Na + N_2O	0	0	0	0.67	0.63	9.55	8.62
Na_2 + N_2O	0	0	0	0.66	0.61	9.10	8.21
NaO + H_2	0	0	0	11.61	10.66	10.46	9.44
NaO + H_2O	18.69	7.06 [c]	11.96	5.80	5.32	4.88	4.40
NaO + CO	2.47	0.93	1.58	5.33	4.89	4.74	4.28
NaO + CO_2	0	0	0	5.40	4.96	4.80	4.33
NaOH + CO_2	0	0	0	4.74	4.35	4.43	4.00

[a] Collision rate constant from long range (R^{-6}) attractive potential:[6, 22, 23]

k(D-D) = $2.826\times10^{-9}\,\mu^{-1/2}\,(\mu_{D1}\,\mu_{D2})^{2/3}\,T^{-1/6}$

k(D-ID) = $1.672\times10^{-2}\,\mu^{-1/2}\,(\mu_{D1}\,\alpha_2^{\,2}+\mu_{D2}\,\alpha_1^{\,2})^{1/3}\,T^{1/6}$

k(Disp) = $2.240\times10^{6}\,\mu^{-1/2}\,((IP_1\,\alpha_2+IP_2\,\alpha_1)(IP_1+IP_2)^{-1})^{1/3}\,T^{1/6}$

[b] Adiabatic Capture – Infinite Order Sudden Approximation (ACIOSA)[24]

k(D-D) = $1.068\times10^{-9}\mu^{-1/2}(\mu_{D\,1}\,\mu_{D\,1})^{2/3}T^{-1/6}$

[c] Stoecklin and Clary[10] applied their Adiabatic Capture - Partial Centrifugal Sudden Approximation method (ACPCSA) to the NaO + H_2O reaction, and obtained a capture rate constant of k (298 K) = 9.06×10^{-10} cm^3 molecule^{-1} s^{-1} (includes a small dispersion contribution).

[d] Long range transition state approximation: energy and total angular momentum-resolved Variational Transition State Theory (μ*J*-VTST).[11]

k(D-D) = $1.809\times10^{-9}\mu^{-1/2}\,(\mu_{D\,1}\,\mu_{D2})^{2/3}\,T^{-1/6}$

k(D-ID)= $1.934\times10^{-2}\,\mu^{-1/2}\,(\mu_{D\,1}\,\alpha_2^{\,2}+\mu_{D\,2}\,\alpha_1^{\,2})^{1/3}\,T^{1/6}$

k(Disp) = $2.021\times10^{6}\,\mu^{-1/2}\,((IP_1\,\alpha_2+IP_2\,\alpha_1)(IP_1+IP_2)^{-1})^{1/3}\,T^{1/6}$

In the expressions above, k is the collision rate constant in cm^3 molecule^{-1} s^{-1}, μ is the reduced mass in g mol^{-1}, μ_D is the electric dipole moment in Debye, α is the electric polarizability in cm^3 and IP is the ionisation potential in eV. Experimental values of the dipole moment, polarizability and ionisation potential are used throughout these calculations if available (see Table S1).

Table S7. Long range attraction rate coefficients (μ*J*-VTST) at 300 K for collisions between adducts and the bath gas (N_2) and corresponding Lenard-Jones parameters [a].

Interaction	***k* (Dipole-Ind. Dipole) /10^{-10} cm^3 molecule^{-1} s^{-1}**	***k* (Dispersion) /10^{-10} cm^3 molecule^{-1} s^{-1}**	**σ /Å**	**ε/K**
$Na(OH)_2 + N_2$	3.50	4.46	4.0	420
$NaCO_3 + N_2$ (N_2O)	4.44 (5.34)	4.79 (5.60)	4.5 [a]	420 [a]
$NaHCO_3 + N_2$	3.75	4.45	4.5	350

[a] Bath gas mixture $0.75\times N_2+0.25\times N_2O$ [13]

Table S8. Experimental and calculated ionisation energies at WU1 level of theory.

	VIE /eV [a]	**AIE /eV**	**Exp. AIE/eV**
Na		5.131	5.1390767 [b]
NaO	7.831 (7.89 [c])	7.535 (7.51 [c])	7.1 [d]
NaOH	8.128 (8.10 [e])	7.845 (7.87 [e])	7.68 [f]
$NaHCO_3$	9.722	8.960	
Na_2		4.885	4.88898 [b]
Na_2O	4.953	4.782	5.06 [g]

[a] Calculated vertical and adiabatic ionisation energies (VIE and AIE respectively) at W1U level of theory. Ab initio literature values in parentheses. [b] Handbook of Chemistry and Physics.[19] [c] CASSCF-MRCI.[25] [d] Onset and maximum of NaO photoelectron band (T ~ 700 K) given respectively as AIE (7.1 eV) and VIE (7.7 eV).[26] [e] RCCSD(T).[27] [f] Onset and maximum of NaOH photoelectron band (T = 920 K) given respectively as AIE (7.68 eV) and VIE (8.11 eV)..[28] [g] PI-QMS (T > 750 K).[29]

Table S9. Fragmentation energies

Fragmentation process	**ΔH_r(298 K) /eV** [a]
$NaO \rightarrow Na^+ + O + e^-$	7.93
$NaO \rightarrow Na^+ + O^-$	6.47
$NaOH \rightarrow Na^+ + OH + e^-$	8.61
$NaOH \rightarrow NaO^+ + H + e^-$	12.84
$NaHCO_3 \rightarrow Na^+ + HOCO_2 + e^-$	9.83 [b]
$NaHCO_3 \rightarrow NaO^+ + HOCO + e^-$	14.05 [b]
$NaHCO_3 \rightarrow NaOH^+ + CO_2 + e^-$	9.21 [b]

[a] From experimental values of the formation enthalpies and ionisation energies of Na, NaO and NaOH and the electron affinity of O. See table S5 for references. [b] This work, at W1U level of theory

D. REFERENCES

(1) Cox, R. M.; Plane, J. M., An experimental and theoretical study of the reactions NaO+ H_2O (D_2O)→ NaOH (D)+ OH (OD). *Phys. Chem. Chem. Phys.* **1999,** *1* (20), 4713-4720.

(2) Frisch, M. J.; Trucks, G. W.; Schlegel, H. B.; Scuseria, G. E.; Robb, M. A.; Cheeseman, J. R.; Scalmani, G.; Barone, V.; Mennucci, B.; Petersson, G. A.; Nakatsuji, H.; Caricato, M.; Li, X.; Hratchian, H. P.; Izmaylov, A. F.; Bloino, J.; Zheng, G.; Sonnenberg, J. L.; Hada, M.; Ehara, M.; Toyota, K.; Fukuda, R.; Hasegawa, J.; Ishida, M.; Nakajima, T.; Honda, Y.; Kitao, O.; Nakai, H.; Vreven, T.; Montgomery Jr., J. A.; Peralta, J. E.; Ogliaro, F.; Bearpark, M. J.; Heyd, J.; Brothers, E. N.; Kudin, K. N.; Staroverov, V. N.; Kobayashi, R.; Normand, J.; Raghavachari, K.; Rendell, A. P.; Burant, J. C.; Iyengar, S. S.; Tomasi, J.; Cossi, M.; Rega, N.; Millam, N. J.; Klene, M.; Knox, J. E.; Cross, J. B.; Bakken, V.; Adamo, C.; Jaramillo, J.; Gomperts, R.; Stratmann, R. E.; Yazyev, O.; Austin, A. J.; Cammi, R.; Pomelli, C.; Ochterski, J. W.; Martin, R. L.; Morokuma, K.; Zakrzewski, V. G.; Voth, G. A.; Salvador, P.; Dannenberg, J. J.; Dapprich, S.; Daniels, A. D.; Farkas, Ö.; Foresman, J. B.; Ortiz, J. V.; Cioslowski, J.; Fox, D. J. *Gaussian 09*, Gaussian, Inc.: Wallingford, CT, USA, 2009.

(3) Steinberg, M.; Schofield, K., A reevaluation of the vaporization behavior of sodium oxide and the bond strengths of NaO and Na_2O: Implications for the mass spectrometric analyses of alkali/oxygen systems. *J. Chem. Phys.* **1991,** *94* (5), 3901-3907.

(4) Ruscic, B.; Pinzon, R. E.; Morton, M. L.; Srinivasan, N. K.; Su, M.-C.; Sutherland, J. W.; Michael, J. V., Active Thermochemical Tables: Accurate Enthalpy of Formation of Hydroperoxyl Radical, HO2†. *J. Phys. Chem. A* **2006,** *110* (21), 6592-6601.

(5) Gurvich, L. V., Reference books and data banks on the thermodynamic properties of individual substances. In *Pure Appl. Chem.*, 1989; Vol. 61, p 1027.

(6) Ager III, J. W.; Howard, C. J., Gas Phase Kinetics of the Reactions of NaO with H_2, D_2, H_2O, and D_2O. *J. Chem. Phys.* **1987,** *87* (2), 921-925.

(7) Glowacki, D. R.; Liang, C.-H.; Morley, C.; Pilling, M. J.; Robertson, S. H., MESMER: An Open-Source Master Equation Solver for Multi-Energy Well Reactions. *J. Phys. Chem. A* **2012,** *116* (38), 9545-9560.

(8) Vasiliu, M.; Li, S.; Peterson, K. A.; Feller, D.; Gole, J. L.; Dixon, D. A., Structures and Heats of Formation of Simple Alkali Metal Compounds: Hydrides, Chlorides, Fluorides, Hydroxides, and Oxides for Li, Na, and K. *J. Phys. Chem. A* **2010,** *114* (12), 4272-4281.

(9) Mintz, B.; Chan, B.; Sullivan, M. B.; Buesgen, T.; Scott, A. P.; Kass, S. R.; Radom, L.; Wilson, A. K., Structures and Thermochemistry of the Alkali Metal Monoxide Anions, Monoxide Radicals, and Hydroxides. *J. Phys. Chem. A* **2009,** *113* (34), 9501-9510.

(10) Stoecklin, T.; Clary, D. C., Fast reactions between diatomic and polyatomic molecules. *J. Phys. Chem.* **1992,** *96* (18), 7346-7351.

(11) Georgievskii, Y.; Klippenstein, S. J., Long-range transition state theory. *J. Chem. Phys.* **2005,** *122* (19), 194103.

(12) Ager, J. W.; Howard, C. J., Rate coefficient for the gas phase reaction of NaOH with CO_2. *J. Geophys. Res. [Atmos.]* **1987,** *92* (D6), 6675-6678.

(13) Ager III, J. W.; Howard, C. J., The kinetics of NaO + O_2 + M and NaO + CO_2 + M and their role in atmospheric sodium chemistry. *Geophys. Res. Lett.* **1986,** *13* (13), 1395-1398.

(14) Millour, E.; Forget, F.; Lewis, S. R. Mars Climate Database version 5.1, http://www-mars.lmd.jussieu.fr/, Oxford, 2014.

(15) Plane, J. M. C.; Husain, D., Determination of the absolute rate constant for the reaction O + NaO → Na + O_2 by time-resolved atomic chemiluminescence at λ = 589 nm [Na(3 ^{2}P) →Na(3 $^2S_{1/2}$) + hν]. *J. Chem. Soc., Faraday Trans. 2* **1986,** *82* (11), 2047-2052.

(16) Plane, J.; Oetjen, H.; de Miranda, M.; Saiz-Lopez, A.; Gausa, M.; Williams, B., On the sodium D line emission in the terrestrial nightglow. *J. Atmos. Sol. Terr. Phys.* **2012,** *74* (0), 181-188.

(17) Griffin, J.; Worsnop, D. R.; Brown, R. C.; Kolb, C. E.; Herschbach, D. R., Chemical Kinetics of the NaO ($A^2\Sigma^+$) + O(^{3}P) Reaction. *J. Phys. Chem. A* **2000,** *105* (9), 1643-1648.

(18) Cox, R. M.; Self, D. E.; Plane, J., A study of the reaction between NaHCO3 and H: Apparent closure on the chemistry of mesospheric Na. *J. Geophys. Res. [Atmos.]* **2001,** *106* (D2), 1733-1739.

(19) Lide, D. R., *Handbook of Chemistry and Physics*. 73 ed.; CRC: Boca Raton, Florida, 1992.

(20) Chase Jr., M. W., *NIST-JANAF Themochemical Tables, 4th ed.* American Institute of Physics: Melville, NY, 1998.

(21) Cox, J. D.; Wagman, D. D.; Medvedev, V. A., *CODATA Key Values for Thermodynamics*. Hemisphere: New York, 1989.

(22) Levine, R. D.; Bernstein, R. B., *Molecular Reaction Dynamics*. Oxford University: New York, 1974; p 46.

(23) London, F., The general theory of molecular forces. *Trans. Faraday Soc.* **1932,** *33* (8).

(24) Clary, D. C., Rates of chemical reactions dominated by long-range intermolecular forces. *Mol. Phys.* **1984,** *53* (1), 3-21.

(25) Soldán, P.; Lee, E. P.; Gamblin, S. D.; Wright, T. G., Photoionization of NaO ($X^2\Pi$; $A^2\Sigma^+$) and the absorption/emission spectra of the lowest cationic states. *Phys. Chem. Chem. Phys.* **1999,** *1* (21), 4947-4954.

(26) Wright, T. G.; Ellis, A. M.; Dyke, J. M., A study of the products of the gas-phase reactions M + N_2O and M + O_3, where M = Na or K, with ultraviolet photoelectron spectroscopy. *J. Chem. Phys.* **1993,** *98* (4), 2891-2907.

(27) Lee, E. P. F.; Wright, T. G., Heats of Formation of NaOH and $NaOH^+$: Ionization Energy of NaOH. *J. Phys. Chem. A* **2002,** *106* (38), 8903-8907.

(28) Dyke, J. M.; Feher, M.; Morris, A., High temperature photoelectron spectroscopy: a study of the alkali monohydroxides LiOH, NaOH and KOH. *J. Electron. Spectrosc. Relat. Phenom.* **1986,** *41* (2), 343-355.

(29) Peterson, K. I.; Dao, P. D.; Castleman, A. W., Photoionization studies of Na_2Cl and Na_2O and reactions of metal clusters. *J. Chem. Phys.* **1983,** *79* (2), 777-783.